Green Chemistry

Solvent Selection for Biphasic Extraction of 5-Hydroxymethylfurfural via Multiscale Modeling and Experiments

Journal:	*Green Chemistry*
Manuscript ID	GC-ART-09-2020-003251.R1
Article Type:	Paper
Date Submitted by the Author:	12-Nov-2020
Complete List of Authors:	Wang, Zhaoxing; University of Delaware, Department of Chemical and Biomolecular Engineering Bhattacharyya, Souryadeep; University of Delaware, Department of Chemical and Biomolecular Engineering Vlachos, Dion; Univ. of Delaware,

Solvent Selection for Biphasic Extraction of 5-Hydroxymethylfurfural via Multiscale Modeling and Experiments

Zhaoxing Wang[#,1,2] Souryadeep Bhattacharyya[#,1,2] and Dionisios G. Vlachos[1,2]*

[1]Department of Chemical & Biomolecular Engineering, University of Delaware, 150 Academy St., Newark, DE 19716, USA
[2]Catalysis Center for Energy Innovation, RAPID Manufacturing Institute, and Delaware Energy Institute (DEI), University of Delaware, 221 Academy St., Newark, DE 19716, USA

# Z.W. and S.B. contributed equally
* Corresponding author: vlachos@udel.edu

Keywords: Biomass, extraction, process intensification, COSMO-RS, solvent design

Abstract

We introduce a comprehensive conceptual framework for selecting solvents for reactive extraction in biphasic organic-water systems and demonstrate it for the separation of HMF (5-hydroxylmethylfurfural), a platform chemical produced in the acid-catalyzed dehydration of hexoses. We first perform *in silico* screening of ~2,500 solvents, from the ADFCRS-2018 database using the ADF COSMO-RS implementation, and classification, based on the solvent partition coefficient. We then determine experimentally the partition coefficients for HMF, fructose, and products of HMF rehydration (levulinic acid (LA), and formic acid (FA)), the mutual water-organic solvent solubilities, and the separation factors in >50 select solvents spanning multiple homologous series at room temperature and a typical reaction temperature with *in-situ* sampling. We find that COSMO-RS is excellent for screening purposes (typical error in most cases within a factor of ~2). Increased temperatures lead to significant reduction in partitioning, and room temperature measurements are clearly inadequate for solvent selection. Upon down selecting classes of solvents based on separation performance, we perform experimental thermal stability and reaction compatibility studies of a small set of solvents at relevant reactive-extraction temperatures. We discover that many substituted phenols exhibit order-of-magnitude increase in partitioning compared to conventional solvents due chiefly to hydrogen bond interactions and show the necessary stability but retain significant fraction of water and LA, factors that need to be considered in technoeconomic analysis. In contrast, anilines, aldehydes, and acids are good to excellent regarding separation but incompatible with this specific reaction media. This multifaceted framework can be extended to other biomass-derived products and processes.

Introduction

Biorefineries based on abundant, domestic, sustainable feedstocks can reduce our dependence (80% of world's energy and 90% of chemicals) on finite, often geographically concentrated, fossil fuel sources, and lower greenhouse gas (CO_2) emissions.[1-4] Economic realization of biorefineries depends on optimal integration of multiple product streams: high volume-low value biofuels with low volume-high value biochemicals, through select intermediates, termed "platform chemicals".[2, 4-6] Among these, furan, 5-hydroxymethylfurfural (HMF), and furfural are important targets.[2, 7] Production of HMF in particular is pivotal for production of valuable products like dimethylfuran (DMF), 2,5-furandicarboxylic acid (FDCA), 2,5-diformylfuran (DFF), 2,5-dihydroxymethylfuran, Bis(5-methylfurfuryl)ether, etc.[1, 5, 8-10]

HMF is produced by acid catalyzed dehydration of C6 monosaccharides (hexoses) or other complex polysaccharides (*e.g.,* sucrose, cellobiose, inulin, cellulose, etc.) *via* hydrolysis to hexoses followed by dehydration.[8, 11, 12] HMF is reactive and undergoes rehydration under acidic aqueous conditions, yielding levulinic acid (LA) and formic acid (FA), and condensation reactions, leading to humins.[11, 13] Suppressing side reactions by partial or complete substitution of the aqueous reaction phase by organic solvents[11, 14-17] (*e.g.,* dimethyl formamide, butanol, dioxane, dimethyl sulfoxide, acetonitrile, etc.) or ionic liquids result in higher HMF yields, [18-22] but water is desirable as it is inexpensive, non-toxic, and has high HMF and substrate (fructose, glucose, etc.) solubility. [23] In addition, sugar dehydration generates water as a by-product and real feed mixtures usually consist of hydrolyzed aqueous solutions.[24] Increasing HMF selectivity can be achieved using biphasic systems with hexose dehydration in water accompanied by selective, *in situ* extraction of HMF to an organic phase.[5, 25, 26] The extraction efficacy is typically quantified by the HMF partition coefficient (P_{HMF}), defined as the ratio of HMF concentration in the organic-rich phase to that in the aqueous-rich phase in an equilibrated biphasic system.[5, 23]

Several biphasic systems utilized for improving HMF yield have been summarized in recent reviews.[25, 26] Dehydration reaction temperatures typically range between 393 K to 453 K and organic to water ratios around 2-4 (v/v). [25] Common extracting solvents include methyl isobutyl ketone (MIBK),[27-30] tetrahydrofuran (THF),[31, 32] 1-butanol,[5, 33, 34] and 2-methyltetrahydrofuran (2-MTHF).[5, 35] Reported P_{HMF} values at room temperature are low (~1-2), necessitating use of large solvent quantities and multiple extraction cycles. Organic solvents with higher P_{HMF} can selectively concentrate the desired product and reduce overall processing costs.

The solvent space is vast and solvent selection is often based on heuristic approaches.[23, 25] Computational methods can be used to estimate activity coefficients of solutes, enabling identification of high performing solvents. COSMO-RS (COnductor-like Screening Model for Realistic Solvation) is one such multiscale model that combines quantum mechanics and statistical mechanics.[36, 37] Unlike group contribution models (*e.g.,* UNIFAC, ASOG, etc.) that utilize empirical group-specific parameters agnostic of the group chemical environment, COSMO-RS accounts for intramolecular interactions. Recently, this approach was extended to HMF extraction at room temperature of ~6,000 solvent-water pairs and revealed alkyl phenols as promising extractants, with subsequent experiments of six solvents showing o-isopropylphenol and o-propylphenol having the highest reported experimental P_{HMF} of 11.9 and 11.5, respectively.[23] In a separate work, COSMO-RS screening on a select solvent dataset identified ethyl acetate (P_{HMF} = 1.33) as a preferred "green" solvent for HMF extraction.[25] Recently, a computer-aided molecular design (CAMD) approach was also proposed to design novel molecules using a genetic algorithm coupled with objective functions based on thermodynamic properties obtained from COSMO-RS and identified phenolic compounds as a class of high-performing solvents for HMF extraction.[38]

Despite considerable literature on HMF extraction, to the best of our knowledge there are a number of gaps. (1) P_{HMF} has always been reported after quenching to room temperature. Significant deviation of phase behavior with temperature may though be expected. High P_{HMF} is desired both at reaction temperature and after cooling; the former being responsible for HMF selectivity and yield during reaction and the latter for increased product concentration in the extracting phase if extraction is done at low temperatures. (2) More extensive validation of COSMO-RS is necessary across different homologous series of solvents to provide an one-stop experimentally validated HMF partition coefficient database to the research community.[23] The accuracy of COMSO-RS for these systems is unclear and needs extensive experimental data. (3) Importantly, solvent selection is a multidimensional optimization problem involving mutual phase solubility data, selectivity of product extraction, and solvent stability, which are all crucial inputs affecting the technoeconomic viability. These points are elaborated below.

In this work, we have comprehensively explored extraction of HMF and relevant species. First, *in silico* screening of mutual water-solvent solubility and HMF partitioning was conducted for over 2,500 solvent/water systems using the ADF COSMO-RS, a two-step model combining QM-based DFT calculations and statistical mechanics. This screening leads to crucial insights into different solvent classes at both ambient (298 K) and reaction relevant temperature (423 K). Second, HMF, fructose, LA, and FA partition coefficients, along with water-organic solubilities for 54 select solvents across different homologous series both at room temperature (298 K) and reaction temperature (423 K) were measured. To the best of our knowledge, this is not only the single largest experimental database of partition coefficients of all relevant components of the hexose dehydration system, but also the first time that partition coefficients of select high performing systems have been experimentally evaluated at reaction temperature. Finally, we propose a conceptual framework to assess the stability and compatibility of solvents and demonstrate this experimentally for the first time.

Materials and Experimental Methods

Materials

The partition coefficients of HMF, LA, FA, and fructose were measured in 54 water/organic systems for validation of the COSMO-RS model. A comprehensive list of the solvents along with relevant information are provided in the Supporting Information (Table S1). ASTM-Type 1 grade deionized (DI) water (Milli-Q® Direct) was used in all experiments.

Quantification of Compounds

HMF was quantified using high-performance liquid chromatography (HPLC) using a Waters e2695 separations module coupled to a Waters 2414 refractive index meter and a Waters 2998 photodiode array detector. An Agilent Zorbax SB-C18 250 mm column was used at 323 K, using a 50/50 (v/v) acetonitrile and water mixture flowing at 0.3 mL/min as the mobile phase. HMF concentration was calculated from the area of its HPLC 254 nm absorbance peak at 8.8 minutes. Fructose, LA, and FA, were quantified using a Bio-Rad Aminex 87H 300 × 7.8 mm column with 5 mM H_2SO_4 at 0.5 mL/min at 323 K. Fructose, FA, and LA concentrations were calculated from the areas of their HPLC refractive index peaks at 12.0, 16.9, and 19.9 min, respectively.

For the solvent stability experiments, solvents were characterized using a GC (Agilent 7890A) with a flame ionization detector (FID) and a HP-Innowax capillary column (30 m × 0.25 mm × 0.25 μm). The GC-FID was coupled to a quantitative carbon detector (QCD, Polyarc) before the

FID, where all carbonic products undergo methanization, allowing product quantification using a unified concentration standard.

Water content in the organic phase was measured using a Mettler Toledo V20 Karl Fischer titrator operating in volumetric mode. The Honeywell Fluka Hydranal Composite 5 two-component titrant was used after concentration determination with DI water. Titration of water-in-ketone standard samples was performed to rule out potential titrant incompatibility with ketones and aldehydes (Table S2). Honeywell Fluka Methanol Dry was used as the working solvent.

Room Temperature Partitioning Studies

A 3 mL of a 1 wt. % aqueous solution of each solute (HMF, fructose, LA, or FA) was mixed with an equal volume of the organic solvent in a 25 mL scintillation vial and stirred at 700 rpm for 3 hr in a temperature-controlled oil bath for equilibration. The equilibration time was determined by analyzing temporal data of 2-chlorophenol, a high performing solvent (Figure S1), to be 20 min. Thus, 3 hr mixing time ensures equilibration across all systems. To determine the effect of fructose concentration on P_{HMF}, a 20 wt. % fructose aqueous solution containing 1 wt. % HMF was also used. After thorough mixing, the equilibrated biphasic solution was centrifuged at 10,000 rpm for 10 min for enhanced phase separation; separate samples were collected from each phase. The partition coefficients were estimated by quantifying the ratio of solute A molar concentration in the organic phase ($C_{\mathrm{A}}{}^{org}$) to the aqueous phase ($C_{\mathrm{A}}{}^{aq}$) through HPLC analysis

$$P_{\mathrm{A}} = \frac{C_{\mathrm{A}}^{org}}{C_{\mathrm{A}}^{aq}} \qquad \textbf{(1)}$$

High Temperature Partitioning Studies

Measurements at elevated temperatures were conducted using a high throughput *in situ* sampling method. As illustrated in Figure S2, a modified Q-tube reactor was setup. After mixing of 1 hr at 700 rpm, a 10-inch needle was used to puncture the septum sealing the Q-Tube. Upon reaching the desired phase, a Luer valve connecting the needle and a syringe was opened and the desired phase was collected and refrigerated. To create a homogeneous phase for analysis, the sample was vortex mixed, immediately transferred to an autosampler vial and diluted with acetonitrile.

A Framework for Assessing Solvent Thermal Stability and Compatibility with Reaction Media

Aside from possessing a high partition coefficient, a good solvent should also be thermally stable and unreactive toward the reactants and products at reaction temperatures. However, little attention has until now been paid to solvent stability and compatibility (reactivity) with HMF at reaction temperatures. Since these metrics cannot be obtained easily computationally, we propose to obtain them experimentally. Given the vast space of solvents, we propose a conceptual hierarchical framework whereby we first screen solvents for separation, using high throughput computations (see below), then classify solvents in homologous series in terms of separation efficacy, and finally select a small number of solvents from various homologous series to test them experimentally for their thermal stability and compatibility in the reaction media. In this manner, the task becomes manageable.

For solvent thermal stability tests, 2 ml pure solvent was added to a Q-Tube reactor, capped and heated to 423 K for 12 hr. Normalized solvent peak areas before and after heating were compared using the GC-Polyarc and a cut-off of 10% change in peak area was used to classify solvents as unstable under reaction temperatures. More stringent criteria, such as higher

temperatures, longer times, and smaller changes in GC area, can obviously be set but the aforementioned values were deemed adequate for an initial evaluation.

Aside from thermal stability, the compatibility of a solvent in the reaction media needs to be evaluated. For example, acetone and related solvents react with the carbonyl group of a furan molecule via aldol condensation under appropriate conditions (usually in a base). Such solvents are not deemed suitable for extraction. For solvent compatibility experiments in the reaction media, two different tests were conducted. First, a room temperature partitioning experiment was conducted. 1.5 ml of the equilibrated organic-rich phase was extracted, added to a Q-Tube reactor, capped, and heated at 423 K for 1 hr. These experiments assess the reactivity of solvent with HMF. For thermal stability and HMF compatibility in the presence of HCl, the same compatibility experiments were performed but the aqueous phase contained 0.25 M HCl. This set of experiments addresses the potential partition of HCl into the organic phase catalyzing reaction of the solvent with HMF. HMF peak areas of the extracted organic phase before and after heating were compared using GC-Polyarc. While the latter set only could have been done, the two sets combined provide understanding of the root cause of solvent incompatibility. Use of a different catalyst, *e.g.*, a hydrophilic solid acid, may not cause acid-catalyzed chemistry in the organic phase. A reduction greater than 10% in the peak area was used to classify a solvent as reactive and unsuitable under reaction conditions. No detailed characterization of the products was conducted as unstable solvents are deemed unsuitable for processing.

Computational Methods

In silico Solvent Screening using COSMO-RS

COSMO-RS is a quantum mechanics/statistical mechanics two-steps model that enables fast first principles' estimation of thermodynamic properties. In its first ("COSMO") step, the molecule of interest is embedded in a virtual, fictitious conductor and its geometry is optimized using density functional theory (DFT). The screening charge density (SCD) surface of the molecule is constructed from the DFT calculation and stored as a COSMO file in a database. In the current work, the TZP small-core basis set, the Becke-Perdew (GGA:BP86) functional, and the scalar ZORA were used for gas-phase geometry optimization of the molecules. The COSMO file is then used to create a distribution of the SCD, known as the σ-profile. The screening charge surface is segmented into areas that interact with each other and the environment. This approximation leads to significant computational savings, as compared to using molecular dynamics where many configurations of the screening charge surfaces would be needed.

The interaction between a pair of surface segments is calculated based on whether there is misfit between the screening charges associated to the pair. When the screening charges cancel out, no energy penalties are applied ("perfectly screened state"). When a misfit does exist, an energy penalty is applied proportional to the size of the surface segments and the square of the charge density difference. In addition, hydrogen bond interactions arise for surface segments carrying high surface charge densities. This brings the σ-profile into context, since it captures the distribution of the screening charge of the surfaces and enables the second COSMO-RS step of statistical mechanics calculations. The chemical potential of a component can thus be calculated.

In this work, *in silico* screening of mutual solubility and partition coefficients of 2,560 water-solvent pairs was conducted using the ADF COSMO-RS implementation in the ADF2019.302 modeling suite with the ADFCRS-2018 database.[39, 40] Water-solvent liquid-liquid equilibria (LLE) were first calculated at 298 K and 423 K, and subsequently used to parametrize partition coefficient calculations for the most stable conformer of the solute (*e.g.*, HMF, LA, and FA) when a

miscibility gap exists. Additional sigma profiles of solvents not in the ADFCRS-2018 database were generated using the recommended setup. The COSMO-RS model and its implementation by ADF can be found elsewhere.[36, 37, 39]

Results and Discussion

Predicted Solvent Solubility and HMF Partitioning at Room and Reaction Temperatures

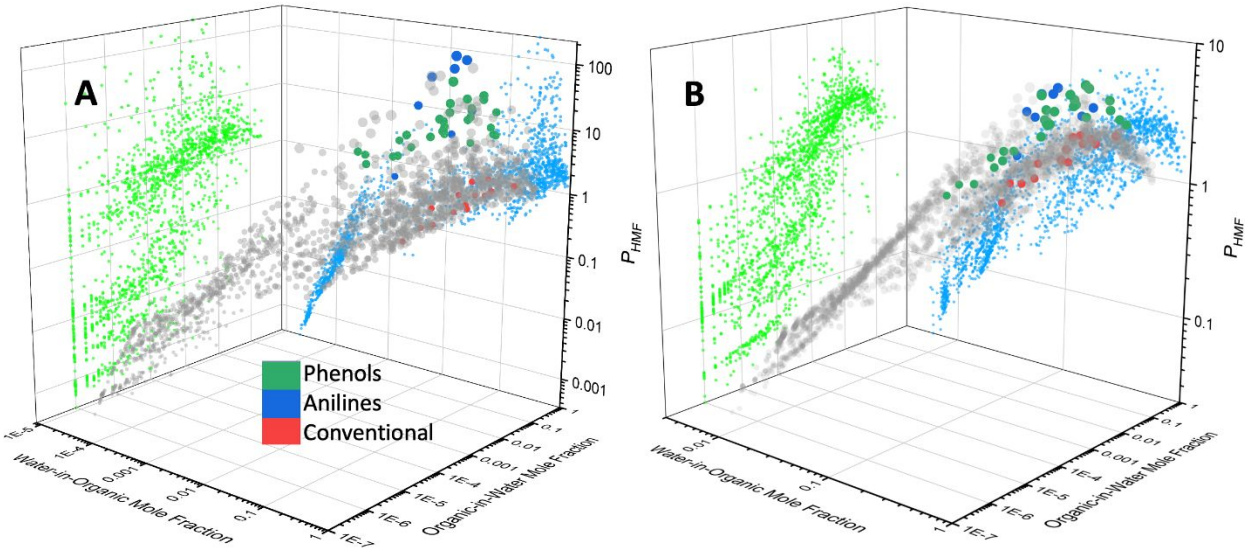

Figure 1. COSMO-RS screening results of solvents for HMF extraction from the aqueous phase at A) 298 K and B) 423 K. Data projections onto the xz (light green) and yz (blue) planes depict the correlation between P_{HMF} and mutual phase solubilities.

The predicted mutual phase solubilities and P_{HMF} at 298 K and 423 K using the COSMO-RS are presented in Figure 1 and the complete results (solvent names, water-in-organic solubility, and organic-in-water solubility, and P_{HMF}) are provided in the SI. Of the 2,560 solvents, 2,215 and 2,195 (excluding ionic liquids) form biphasic systems at 298 K and 423 K, respectively. COSMO-RS assumes that the solvent is liquid at a specified temperature, and thus, the melting points of the solvents chosen for experiments were checked. For example, low-melting solids, such as 3-chlorophenol and o-cresol, form stable liquid-liquid biphasic systems with water at room temperature.

We classify the solvents based on the value of P_{HMF} into three categories: Poor solvents with $P_{HMF} < 1$ that are unsuitable for extraction; typical or conventional solvents used successfully in most prior work with $1 < P_{HMF} < 2$, and high performing solvents with $P_{HMF} > 2$ or ideally >> 2. Compared to prior work in an unsalted aqueous phase using solvents of $P_{HMF} < 2$,[5, 23] 80 solvents have $P_{HMF} > 10$ at 298 K. These consist mainly (75%) of aromatic substituted amines, such as anilines, phenols, and a few substituted organic acids. Clearly a number of high extraction performance solvents exist. An interesting feature revealed in Figure 1A is that significant amount of water can exist in the organic phase, i.e., $x_w^{org} > 0.1$ and often >> 1; the converse is less often true, i.e., $x_{org}^{w} < 0.1$ in most cases. Here x_A^B stands for the mole fraction of A in phase B. The projection of P_{HMF} data on the organic-in-water solubility plane (green points) indicates several high performing solvents (80 solvents with $P_{HMF} > 10$) at 298 K, with 79% of them having a low mole fraction x_{org}^{w} in the range 10^{-4} to 10^{-2}, which implies that downstream separation load of the

aqueous stream is low. On the contrary, P_{HMF}-projected data on the water-in-organic solubility plane (blue points) is concentrated, with 93% having a high water-solubility in the organic phase of $x_w^{org} > 0.1$. For $P_{HMF} > 5$ (set of 150 solvents), 91.3% of the solvents have $x_w^{org} > 0.1$. Conversely, solvents with low water-in-organic solubility (*e.g.,* non-polar hydrocarbons) exhibit $P_{HMF} << 1$. The high solubility of water-in-the organic phase has been overlooked in the past, especially for high performing solvents, and needs to be considered in downstream separations as the organic stream contains a relatively large fraction of water.

The $P_{HMF} > 1$ data indicates an overall positive correlation between P_{HMF} and the water solubility in the organic phase, with P_{HMF} first rising with increasing solubility and then decreasing at high solubility, giving a volcano-like shape. Significant scatter from a perfect linear correlation indicates that the extraction is correlated but is not governed exclusively by the water solubility in the organic solvent. We further discuss this point below.

As the temperature increases, the mutual solubilities of most solvent-water pairs increase (Figure 1B and Figure S3A-B), whereas P_{HMF} increases strongly for weak extractants ($P_{HMF} << 1$) but reduces dramatically for high performers ($P_{HMF} >> 1$, Figure S3C). The number of highly extracting solvents drops from 219 at 298 K to 6 at 423 K (Figure 1B). This strongly suggests that the measured P_{HMF} after quenching the dehydration reaction is significantly higher than that at reaction temperatures and the temperature dependence needs to be considered for designing the reactive extraction process. Furthermore, P_{HMF} measured at room temperature is not indicative of that at reaction temperatures and *in situ* measurements are necessary.

Experimental Assessment of Model Predictions at Room Temperature

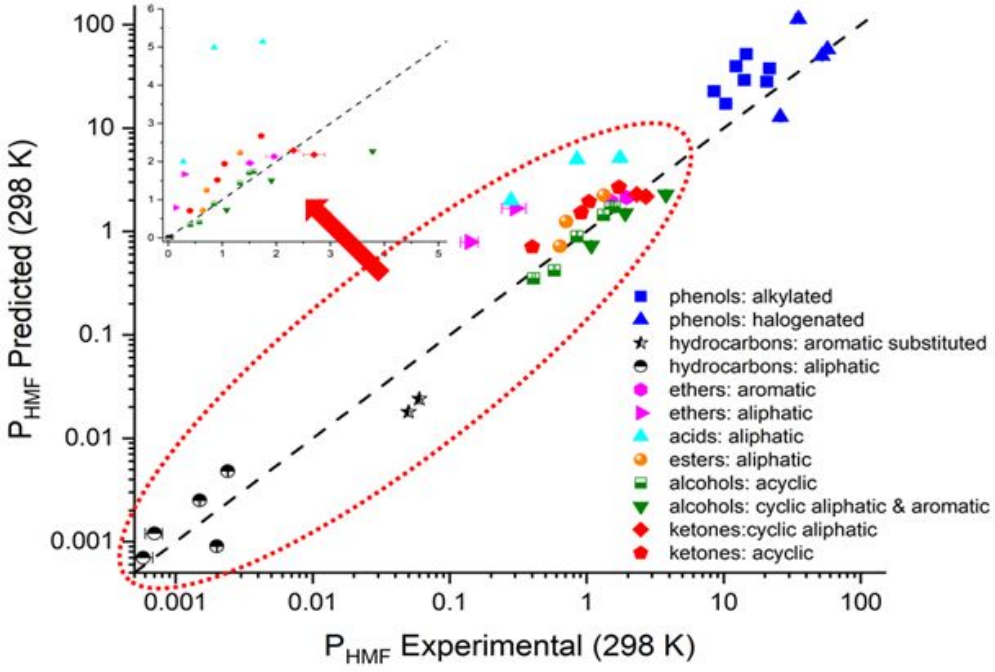

Figure 2. Parity plot of experimental vs. predicted P_{HMF} at 298 K. Conventional solvents used in HMF extraction and low-performing hydrocarbons are shown in magnification in the inset.

To assess the COSMO-RS predictions, P_{HMF} was estimated experimentally for 54 solvents from multiple homologous series summarized in the legend of Figure 2 and in more detail Table

S4. Most predictions differ from experimental values by less than a factor of 2, consistent with the reported error of COSMO-RS.[36] Aliphatic and aromatic hydrocarbons possess $P_{HMF} < 0.1$. Aromatic hydrocarbons exhibit an order of magnitude higher P_{HMF} than aliphatic alkanes (10^{-2} vs 10^{-3}) possibly due to pi-pi interactions with the furan ring. Obviously, these solvents are unsuitable for extraction. Typical solvents for HMF extraction, such as alcohols, ethers, and ketones (*e.g.,* MIBK, 1-butanol), have been used successfully but have modest P_{HMF}~1-2.[5, 10, 41] As the carbon chain-length increases, P_{HMF} decreases due to decreasing solvent polarity. Short chain (C < 4) solvents form monophasic systems (Table S4).[5] In this regard, intermediate size solvents are best in striking a balance between solubility and extraction. Cyclic aliphatic solvents in each homologous series have higher P_{HMF} than the corresponding aliphatic counterparts. For example, P_{HMF} is 2.32 for cycloheptanone vs. 0.91 for heptanone and 1.91 for cyclopentanol *vs.* 1.33 for 2-pentanol. Cyclohexanone has the highest P_{HMF} of 2.7. Substituted phenols, such as m-cresol, 2-isopropylphenol, exhibit excellent $P_{HMF} > 10$. Cresols (methyl phenols) exhibit a higher P_{HMF} ~20 than longer alkyl chains, *e.g.*, 2-ethylphenol (15), 2-isopropylphenol (12), 2-sec-butylphenol (9) and phenol itself ($P_{HMF} = 14$). Halogenated phenols, *e.g.*, 3- and 4-chlorophenols, exhibit the highest P_{HMF}, *e.g.*, 57.1 and 52, respectively. To the best of our knowledge, this is the highest reported experimental P_{HMF} to date and agrees well with COSMO-RS predictions. Predicted high-performing anilines are reactive with HMF (Figure S4) and are ruled out (see also discussion below).

The inset in Figure 2 reveals large deviations (overpredictions) in P_{HMF} for aliphatic acids, *e.g.*, pentanoic acid. Systematic overpredictions are also observed for LA and FA species (Figure S5). This is probably due to the unaccounted deprotonation of acids in COSMO-RS calculations and is worth of further investigation. As discussed below, these solvents are not suitable for this application and are not investigated in detail.

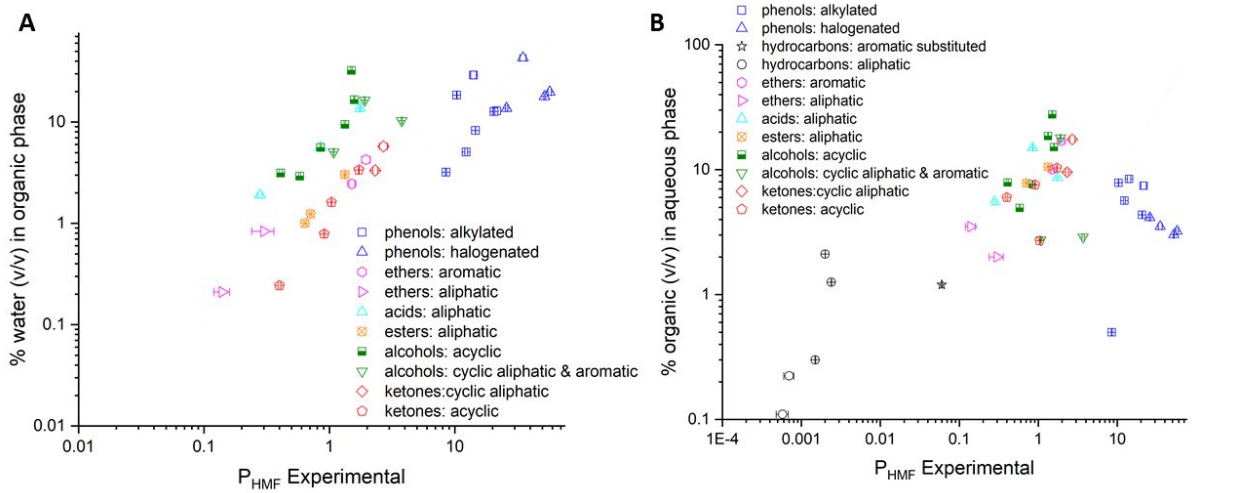

Figure 3. Water content vs. P_{HMF} in the organic-rich phase (A) and organic content in the aqueous-rich phase (B) inferred from experiments at 298 K. No water could be detected in the organic-rich phase for hydrocarbons (not shown in (A)). Note that in cases with low error, the error bars overlap with their symbols.

The mutual solubility of the aqueous and organic phases for all 54 solvent-water pairs is compared with the corresponding solute partition coefficients in Figure 3 (see also Figure S8 and Table S4). Tables S3 and S4 show that nearly insoluble (water undetectable by KF) aliphatic and aromatic hydrocarbons exhibit extremely low P_{HMF}. Figure 3 has less data than Figure 1 and trends are easier to discern. It more clearly shows that within a homologous series of solvents, a positive

correlation exists whereby the higher the water content in the organic phase, the higher the HMF fraction is. Alcohols stand out due to their high solubility with water making the alcohol phase rich in water but relatively poor in HMF content (high $x_{\mathrm{w}}^{\mathrm{org}}$ but low $x_{\mathrm{HMF}}^{\mathrm{org}}$; Figure 3A). Overall, the solubility of water in a homologous series of organic solvents is a primary descriptor of HMF partition but the chemical nature of the homologous series of solvents also matters.

Primary alcohols and cyclic ethers have relatively high solubility (v/v) in the aqueous phase, *e.g.*, 2-butanol (27%), 2-pentanol (18%), 1-butanol (15%), 2-MTHF (17%), indicating high solvent loss per extraction cycle in the absence of solvent recycling from the raffinate stream. High performing solvents have considerably lower solubility in water, *e.g.*, 2-sec-butylphenol (0.5%) and chlorophenols (3-4%). Given their high P_{HMF} values, these solvents are promising candidates for extraction. Figure 3 thus serves as an important guide for solvent selection highlighting trade-offs between high P_{HMF} and solvent solubilities that affect downstream separation and techno-economics.

In summary, except for acids that dissociate and are reactive solvents, COSMO-RS is a semiquantitative tool (error within a factor of 2) and capable of screening organic solvents. Alkylated phenols of modest alkyl chain-length and halogenated phenols exhibit superior partition coefficient. Anilines are reactive with HMF and unsuitable for this application. The solubility of water in organic solvent correlates strongly with the HMF partition.

Effect of Fructose on HMF Partition

Use of concentrated aqueous fructose solutions is desirable for high HMF productivity but leads to increased humin formation.[11, 25] Concentrated fructose has been reported to promote HMF and LA partition into 2-MTHF, 1-butanol, and 2-butanol.[23] Therefore, it is important to understand how generic this effect is. The results for 20 wt.% fructose for select 27 high performing solvents are shown in Figure 4 (see also Table S3 and Figure S7). For this list, we removed solvents from the original list of 54 that are reactive (7) (*e.g.*, aniline), form a single-phase (4) (*e.g.*, dioxane), and consist of peroxide forming ethers (2), extremely low partitioning (7) (*e.g.*, pentane) along with the lowest performers (P_{HMF} <1) within each homologous series (*e.g.*, decanone). Pentafluorophenol (P_{HMF} = 35) was not evaluated further due to potential release of HF upon heating. Fructose indeed enhances P_{HMF} on average by 16% for typical solvents and more so for cyclic ketones, *e.g.*, for cycloheptanone by 35%. The effect is less pronounced in carboxylic acids and ethers. The effect of fructose concentration on P_{HMF} for phenolic solvents is complex. For some alkyl phenols, such as 2-sec-butylphenol and 2-isopropylphenol, P_{HMF} increases (7-21%), but decreases for cresols (methyl phenols) and chlorophenols by 1.5-13% (Figure S7A). Given the large variation of the partition coefficient among solvents, the effect of fructose is of second order. Fructose reduces somewhat water solubility in the organic phase (Figure S7B and Table S4), an effect that should be considered in overall process evaluation.

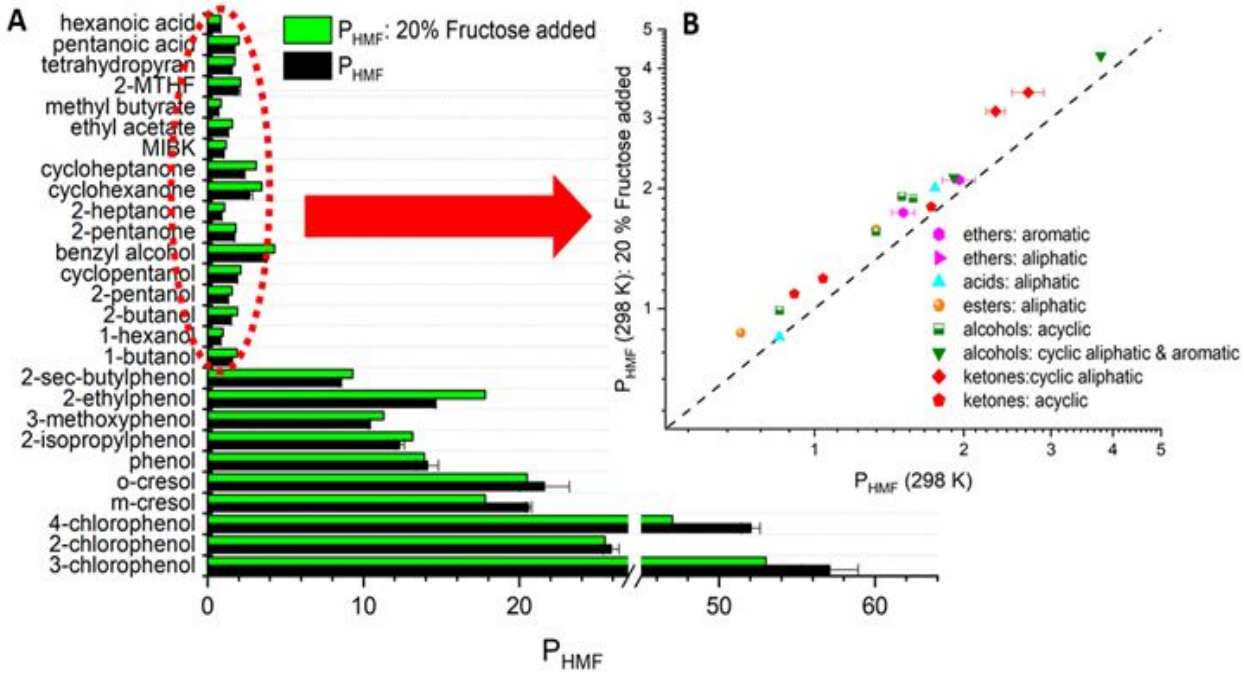

Figure 4. Effect of fructose addition (20 wt.%) on P_{HMF} (A) and parity plot of fructose effect in typical solvents at 298 K (B).

Partitioning of Other Solutes at Room Temperature

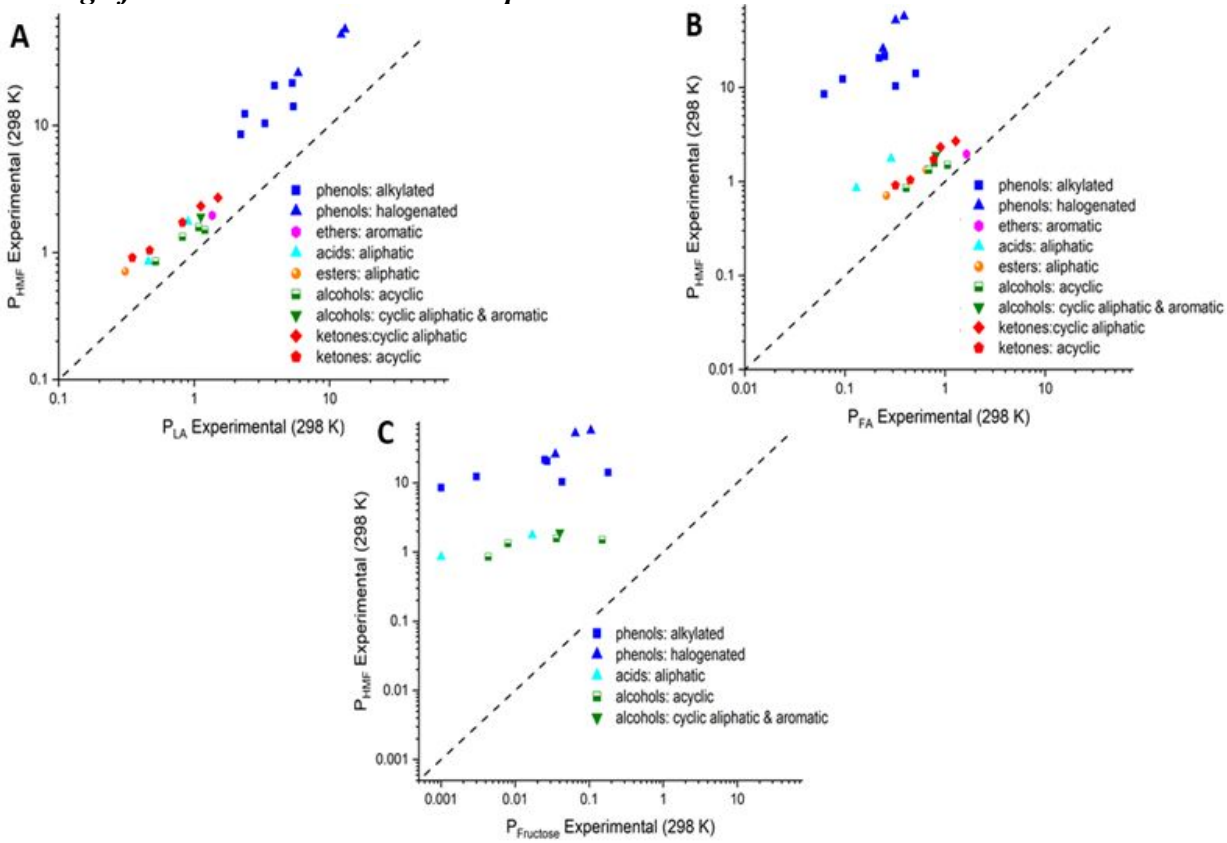

Figure 5. Parity plots of experimental A) P_{HMF} vs. P_{LA}, B) P_{HMF} vs. P_{FA}, and C) P_{HMF} vs. $P_{Fructose}$ at 298 K.

Aside from HMF, the substrate fructose as well as LA and FA, the HMF rehydration products, play a role in downstream separations. Since fructose and HMF can undergo reversion, dehydration and rehydration reactions in acidic aqueous solutions (e.g., LA, FA solution), partitioning experiments in dual solute mixtures with LA or FA were not conducted. While separation factors from individual partitioning experiments with dilute solutes (1 wt. %) may not account for possible solute-solute interactions in concentrated reaction mixtures, our experimental P_{HMF} for typical extractants are in agreement with literature's from fructose dehydration experiments in the presence of acids (after quenching).[5] This is probably due to the fact that LA and FA are relatively weak acids and dehydration happens using strong Bronsted acids.

For the remaining of the work, we focus on the 27 high performing solvents. The separation factor α (ratio of partition coefficients of two extractable solutes) is used as a metric in quantifying the selectivity of an organic solvent in extracting HMF. The experimentally determined $P_{Fructose}$, P_{LA} and P_{FA} are shown in Figure 5 and the separation factors are listed in Table 1. P_{HMF} is greater than that of all other species. A strong correlation is observed for P_{HMF} with P_{LA}, attributed to the chemical similarity of HMF and LA (Figure 5A); this correlation also holds across the COSMO-RS dataset (Figure S6). This implies that a significant fraction of LA partitions into the organic phase. Substituted phenols exhibit comparable $\alpha_{HMF/LA}$ ~ 2-5 to that of conventional solvents (Figure 5A).

Unlike LA, FA exhibits low partitioning into the organic phase for most solvents. The data clusters into two distinct groups, namely the substituted phenols and other solvents. An overall positive correlation of HMF and FA is seen (Figure 5B). Clearly, FA, with its short chain length, prefers to be in water. $\alpha_{HMF/FA}$ is relatively high in phenols and low in typical solvents. P_{LA} and P_{FA} correlate well with the water solubility in the organic phase (Figure S8A-B).

HMF and fructose partition coefficients are not correlated (Figure 5C). Fructose minimally partitions into the organic phase ($P_{Fructose}$~0.001-0.1), leading to a high $\alpha_{HMF/Fructose}$ (100-1000). $\alpha_{HMF/Fructose}$ in 2-butanol, 1-butanol, cyclopentanol, and phenol are high (10-100) and fructose is not detectable in many organic solvents (*e.g.*, ketones, esters etc.). Overall, despite the high solubility of water in organic solvents, fructose partitioning in the organic phase is low. Unlike other solutes, $P_{Fructose}$ is very well correlated with the water-in-organic solvent solubility (Figure S8C, B, Figure S9, Table S3, and Table S4) indicating the sugars being very hydrophilic are probably being entrained by water in the organic phase.

Table 1. Separation factors of species associated with fructose dehydration with respect to HMF at 298 K and 423 K.

	Solvent	Separation Factor (HMF:Fructose)		Separation Factor (HMF:LA)		Separation Factor (HMF:FA)	
#		298 K	423 K	298 K	423 K	298 K	423 K
1	2-isopropylphenol	4107	281	5.2	2.4	129.7	20.7
2	3-chlorophenol	541	60.4	4.4	2.6	146.4	33.0
3	2-chlorophenol	740	76.7	4.4	2.1	107.9	14.8
4	3-methoxyphenol	241.2	SP*	3.1	SP	32.4	SP
5	2-ethylphenol	2217	184.5	3.5	2.3	86.5	17.5
6	2-sec-butylphenol	8500	280.0	3.85	1.75	137.1	20.5
7	phenol	78.3	SP	2.6	SP	27.7	SP

8	4-chlorophenol	800.5	55.3	4.3	3.5	162.6	21.1
9	1-butanol	43.9	SP	1.5	SP	2.0	SP
10	1-hexanol	196.8	61.7	1.6	1.5	2.1	2.9
11	2-pentanone	∞	261.3	2.10	1.8	2.2	2.8
12	2-heptanone	∞	NE*	2.6	NE	2.8	NE
13	cyclohexanone	∞	35.5	1.8	1.7	2.1	2.9
14	cycloheptanone	∞	137.2	2.1	2.0	2.6	3.7
15	MIBK	∞	620.3	2.2	2.0	2.3	3.0
16	2-butanol	10	SP	1.3	SP	1.4	SP
17	2-pentanol	166.3	33.5	1.6	1.2	2.0	2.0
18	ethyl acetate	∞	151.3	NE	NE	2.1	1.5
19	methyl butyrate	∞	401.1	2.3	1.8	2.7	2.6
20	cyclopentanol	47.8	6.2	1.7	1.3	2.4	2.0
21	benzyl alcohol	320	14.2	2.1	1.6	7.7	4.3
22	2-MTHF	∞	285.5	1.4	1.3	1.2	1.8
23	tetrahydropyran	∞	385.6	1.50	1.4	1.5	2.2
24	pentanoic acid	102.9	NE	1.9	NE	6.0	NE
25	hexanoic acid	850	NE	1.9	NE	6.5	NE
26	m-cresol	763.0	22.9	5.3	1.7	93.6	8.9
27	o-cresol	864	69.4	4.1	2.1	86.4	13.8

*: SP = single phase, NE = not evaluated.

Experimental Data and Model Assessment at High Temperatures

Given that dehydration reactions are typically carried out at higher temperatures (~423 K) and P_{HMF} values are reported after quenching the reaction, we have estimated P_{HMF}, P_{LA}, P_{FA} and $P_{Fructose}$ for select solvents, listed in Table 1, using an *in situ* phase sampling method for the first time (see Methods). Monophasic systems at 423 K (phenol, 3-methoxyphenol, 1-butanol, and 2-butanol), carboxylic acids (stability considerations; see stability section later), and the low-performing 2-heptanone (P_{HMF} = 0.9) were not evaluated for high temperature P_{HMF}. The high temperature sampling enables quantification of composition in both phases at reaction temperature and eliminates interphase mass transfer effects associated with quenching.

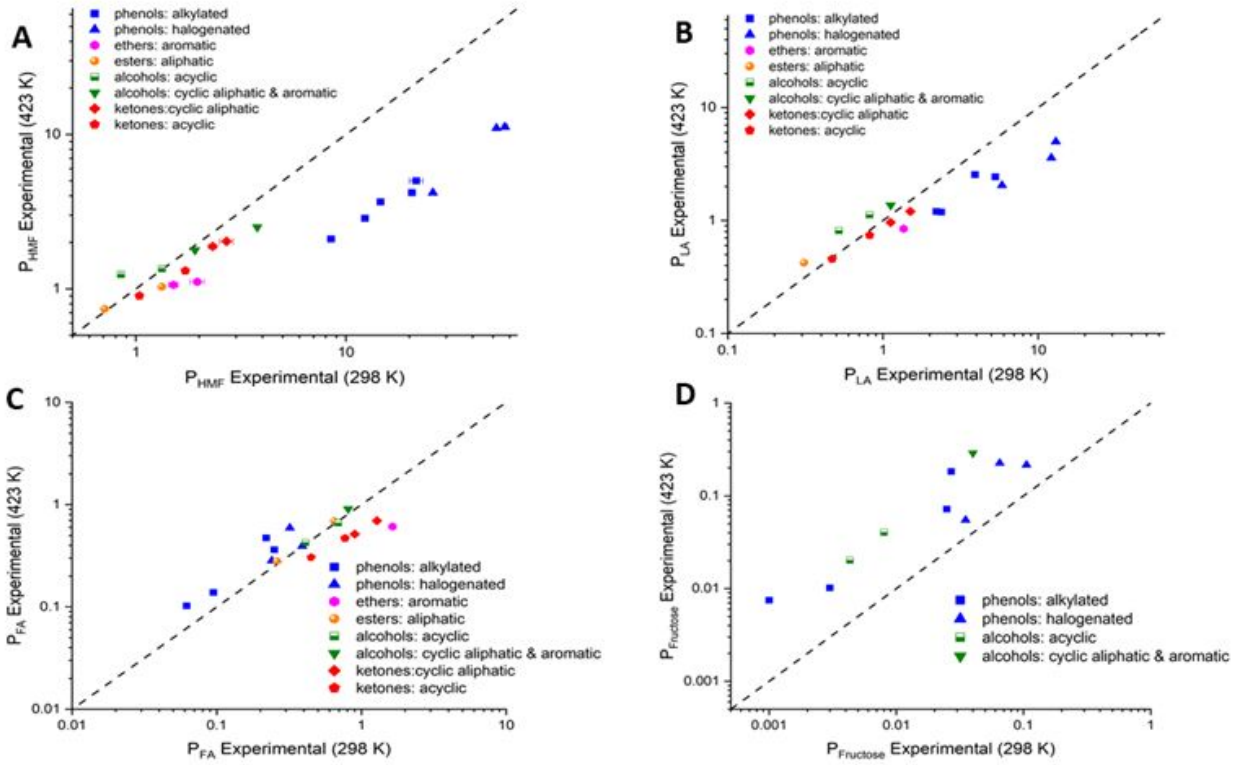

Figure 6. Parity plots of experimental A) P_{HMF}, B) P_{LA}, C) P_{FA}, and D) $P_{Fructose}$ at 298 K *vs.* 423 K data.

The experimental partition data at 423 K is in good agreement with the predicted P_{HMF} (Figure S10). Errors are usually within a factor of 2 and only occasionally higher. Phenols are still the best performing solvents. P_{HMF} for phenolic solvents drops with increasing temperature (Figure 6A), e.g., from 57 to 13 for 3-chlorophenol. This effectively shrinks the selection space for HMF extractants at reaction temperature, consistent with COSMO-RS predictions (Figure 1B). Most of the typical solvents exhibit lower P_{HMF} with increasing temperature, whereas 1-hexanol and methyl butyrate exhibit a minor increase (Table S3). Similar observations hold for P_{LA}, consistent with the strong correlation between P_{HMF} and P_{LA} at all temperatures (Figure 5A, Figure S11A). Minor changes are observed for P_{FA} at 423 K with an increase in phenolics but a reduction in typical ketones and ethers (Figure 6C). All solvents exhibit increased $P_{Fructose}$ at 423 K (Figure 6D). However, the low $P_{Fructose}$ values (< 0.3) even at 423 K indicate its strong preference for the aqueous phase. The separation factors $\alpha_{HMF/Fructose}$ and $\alpha_{HMF/FA}$ decrease substantially at high temperatures while $\alpha_{HMF/LA}$ exhibits a minor decrease (Table 1, Figure 7). Importantly, separation factors for HMF over other solutes is always greater than 1 implying selective extraction at reaction temperatures.

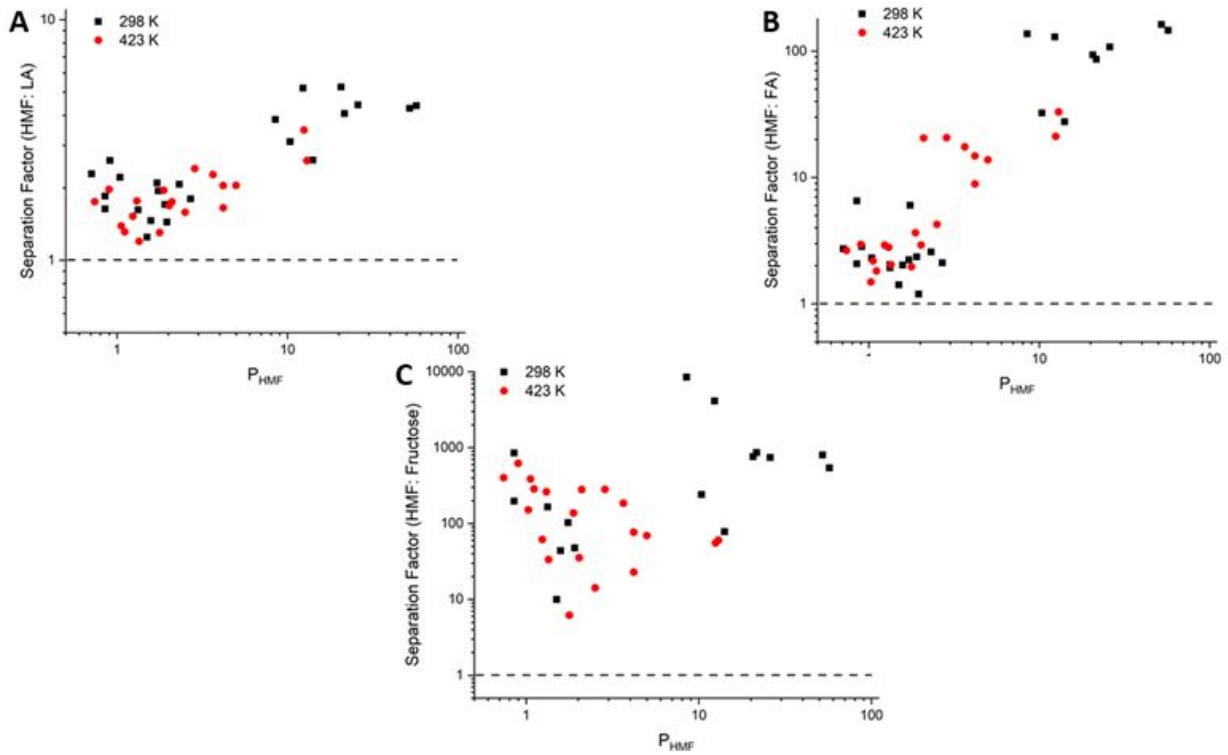

Figure 7. Scatter plots of separation factors for A) HMF:LA, B) HMF:FA, and C) HMF:fructose at 298 K and 423 K.

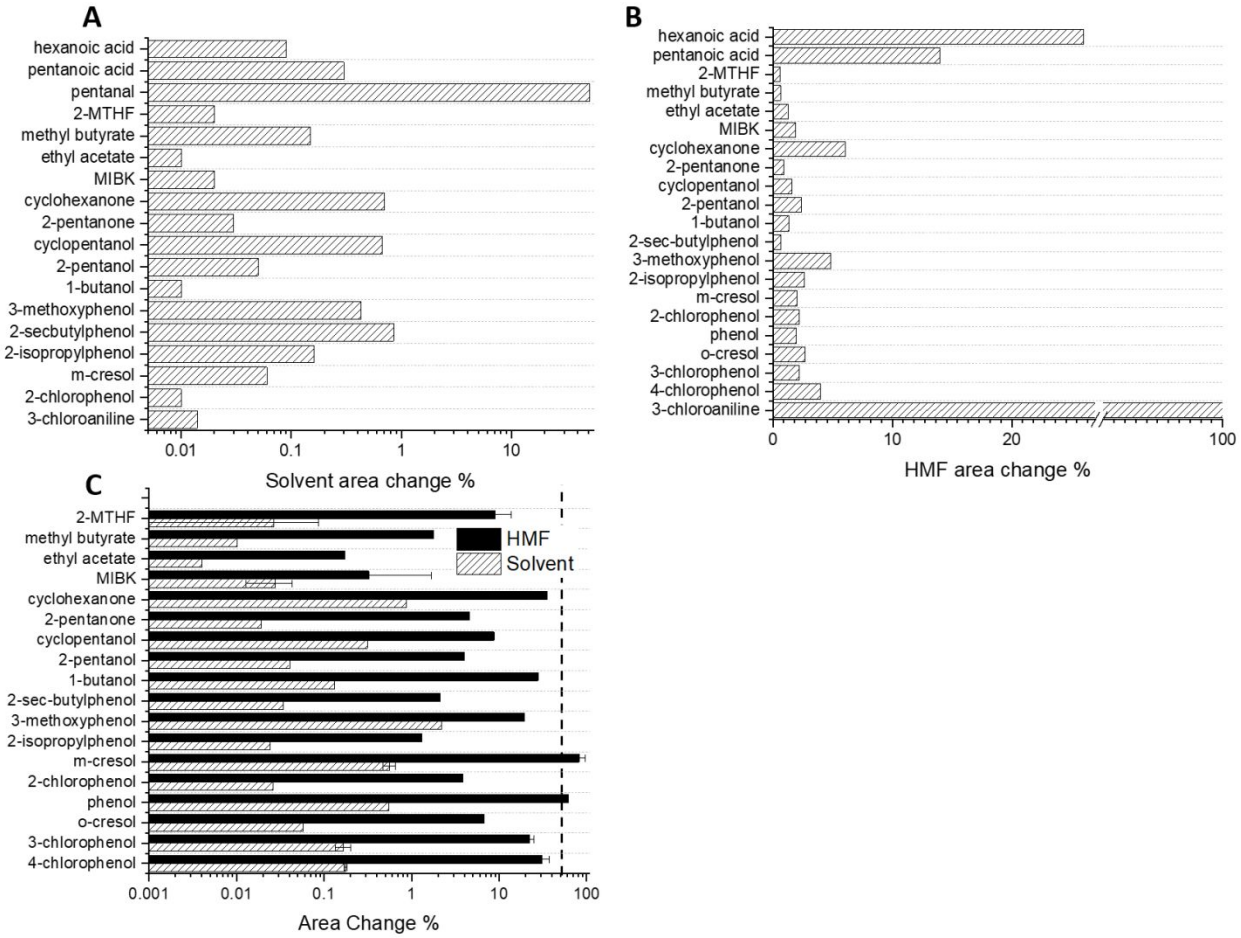

Figure 8. Percent change in normalized peak area at 423 K of A) pure solvents heated for 12 hr and B) equilibrated organic-rich phase of solvent-water-HMF ternary systems heated for 1 hr, and C) equilibrated organic-rich phase with aqueous solution of 1 wt% HMF and 0.25 M HCl, heated for 1 hr. The dashed line in panel C indicates HMF consumption of 53% in 0.25 M HCl at 423 K for 1 hr.

Solvent Stability and HMF Compatibility Experimental Data

In screening solvents for reactive extraction, it is important to ensure their stability and compatibility in the reaction media under extraction conditions. A subset of solvents across multiple homologous series was chosen to evaluate their thermal stability upon heating at 423 K for 12 hours. The GC solvent peak areas before and after heating were compared (Figure 8A). Phenol, 3-chlorophenol, 4-chlorophenol, and o-cresol, are solids at 298 K and were not tested. Of the solvents selected, spanning across homologous groups, all except for pentanal showed less than 1% change upon heating.

In a second set of experiments, the compatibility of the solvent with HMF was evaluated. The organic solvent was equilibrated with an aqueous solution containing 1 wt.% HMF at room temperature followed by extraction of the organic-rich phase and heating at 423 K for a short time of 1 hr. The reactivity of the solvent with the extracted HMF and water was analyzed by comparing the HMF peak area (GC and HPLC) before and after heating (Figure 8B). Of the solvents investigated, the HMF peak area in carboxylic acids decreased more than 15%, indicating HMF reactivity at high temperatures, while in other solvents the changes were < 6%. In substituted anilines, a strong reduction in HMF peak area and new peaks were observed even at 298 K, suggesting high reactivity of the amine groups with HMF (Figure S4).

Next, the solvent-HMF compatibility was evaluated with organic solvents pre-contacted with 0.25 M HCl and 1 wt% HMF aqueous phase, while keeping other conditions identical to the second set. An aqueous solution (0.25 M HCl, 1 wt.% HMF) was heated at 423 K for 1 hr and the HMF loss was quantified (53%) as a baseline for a monophasic aqueous system. Based on the second set, we excluded carboxylic acids and 3-chloroaniline. While change in the normalized solvent area with HCl was low (< 3%) for all solvents, the HMF reactivity varied significantly. Most notable HMF loss occurred in m-cresol (80±10%) and phenol (61%), exceeding the baseline. On the other hand, o-cresol, 2-chlorophenol, and longer chain alkylphenols appear highly compatible (<10% area change) with HMF. Therefore, we conclude that substituted anilines, select phenols, aldehydes, and carboxylic acids are unsuitable for HMF reactive extraction from aqueous solutions.

It has been reported that phenols can undergo condensation reactions with HMF in the presence of Lewis acids ($CrCl_2$/$CrCl_3$) in tetraethyl ammonium chloride (TEAC) at long times (> 4 hr),[42] but our data on fructose dehydration indicate that several phenols do not react with HMF, in agreement with previous literature.[43, 44] Some phenols can be derived from lignin.[45] However, their adoption is not straightforward as they are toxic and high boiling solvents, requiring high temperatures for HMF separation via distillation, and may create product stewardship challenges for certain applications.[43] To quantify the suitability of a solvent, safety, health, and environment criteria for solvents giving biphasic systems were determined based on their physical properties and GHS statements, using the CHEM21-based solvent selection recommendations. The results are shown in Table S4. [46] Phenolic solvents have a favorable score for safety but not for health and environmental criteria, attaining an overall problematic (P) or hazardous (H) recommendation. This highlights the need for solvent selection based on multiple criteria using a multi-objective optimization including technoeconomic analysis.

Insights into Physicochemical Interactions of High Performing Solvents

Solute-solvent interactions of several phenolics make them exceptional for this application. It may be hypothesized that *pi-pi* interactions between aromatic rings of the solute and the solvent result in high P_{HMF}. However, other aromatic solvents, *e.g.,* toluene, exhibit low partition coefficient. In addition, aromatic halogenated groups cannot solely account for the high P_{HMF} of chlorophenols (57), as evidenced by the low value in chlorobenzene (0.06). Similarly, aliphatic alcohols and benzyl alcohol exhibit modest P_{HMF} ~1-2 and 3.8, respectively, whereas phenol and cresol have a high P_{HMF} of 14 and 20, respectively. The benzene ring directly bonded to a -OH group gives a high P_{HMF}. Among substituted phenols, the methyl group (cresol) results in increased P_{HMF} but further increase in alkyl group chain length progressively decreases P_{HMF}. This likely results from increased hydrophobicity by the non-polar alkyl groups, as observed for aliphatic alcohols.[5] High P_{HMF} of chlorophenols (2-4 times more than phenol) may be attributed to electron withdrawing -Cl groups that increase the ability of the -OH group to act as a hydrogen bonding (HB) donor, leading to superior partition coefficients.

The observations above, along with the significantly lower (75-85%) P_{HMF} in substituted phenols at 423 K, lead to the hypothesis that favorable HB interactions between HMF and solvent molecules in the organic-rich phase lead to efficient separation. The COSMO-RS interaction energy functional for molecular surfaces (Eq. 2) includes a separate HB term apart from the electrostatic misfit energy interactions that allows analysis of contributions of all components[37, 47]

$$e(\sigma,\sigma') = \frac{\alpha'}{2}(\sigma+\sigma')^2 + c_{hb}f_{hb}(T)\min\left(0,\min\left(\sigma,\sigma'\right)+\sigma_{hb}\right)\max\left(0,\max\left(\sigma,\sigma'\right)-\sigma_{hb}\right) \quad (2)$$

In this equation, the HB interaction is only included if the screening charge density of the surface segment, σ or σ', exceeds a threshold value set empirically (σ_{hb}). This HB contribution is

temperature dependent and varies with the HB interaction coefficient (f_{hb}) (Eq. 3), showing that HB contributions diminish at higher temperatures

$$f_{hb}(T) = \frac{T \ln\left(1 + \frac{1}{200}\exp\left(\frac{20\ \text{kJ/mol}}{kT}\right)\right.}{298.15\ \text{K} \ln\left(1 + \frac{1}{200}\exp\left(\frac{20\ kJ/mol}{k298.15K}\right)\right.)} \quad (3)$$

We thus performed COSMO-RS calculations with (1) HB contributions left out at 298 K and (2) with HB interactions on but without temperature dependence (f_{hb} = 1) at 423 K; the results are shown in Figure S13. For case 1, P_{HMF} decreases for most solvents of $P_{HMF} > 1$ and more so for substituted phenols (decline of > 90%), providing support for phenol-HMF HB interactions. For case 2 (Figure S13B), P_{HMF} remains largely unchanged for most solvents with $P_{HMF} < 1$, while substituted phenols again experience the largest changes in P_{HMF}. This further supports that favorable solvent-HMF HB interactions contribute toward the high P_{HMF} values.

To further study HMF-solvent interactions, we selected four organic solvents in their respective equilibrated organic-rich phase, with binary equilibrium compositions calculated by ADF COSMO-RS at 298 K. The sigma potential is a measure of pseudo-chemical potential experienced by a molecular surface segment carrying a specific surface charge density. We compared the sigma profile of HMF with those of 3-chlorophenol (high P_{HMF}), benzyl alcohol (medium P_{HMF}), 2-pentanol (conventional solvent with low P_{HMF}), and toluene (very low P_{HMF}) in Figure 9. Toluene exhibits a parabolic shape with positive chemical potentials for polar ($|\sigma| > 0.01$ e/Å^2) surface segments, indicating unfavorable solvent interactions of these segments of HMF and water. This is consistent with the low water-in-organic solubility and low P_{HMF} in toluene. Conversely, 3-chlorophenol, benzyl alcohol, and 2-pentanol show downward sigma potential as surface segments become increasingly polar, with the sigma potential dropping below -0.2 kcal/mol/Å^2 for surface charge densities at 0.015 e/Å^2 for 3-chlorophenol, where significant HMF surface segments are present. Similarly, the sigma potential of benzyl alcohol and 2-pentanol is between zero and -0.1 kcal/mol/Å^2 for surface charge densities near 0.015 e/Å^2, creating less favorable interaction with HMF surface segments. These qualitative trends are consistent with the HB interaction analysis above.

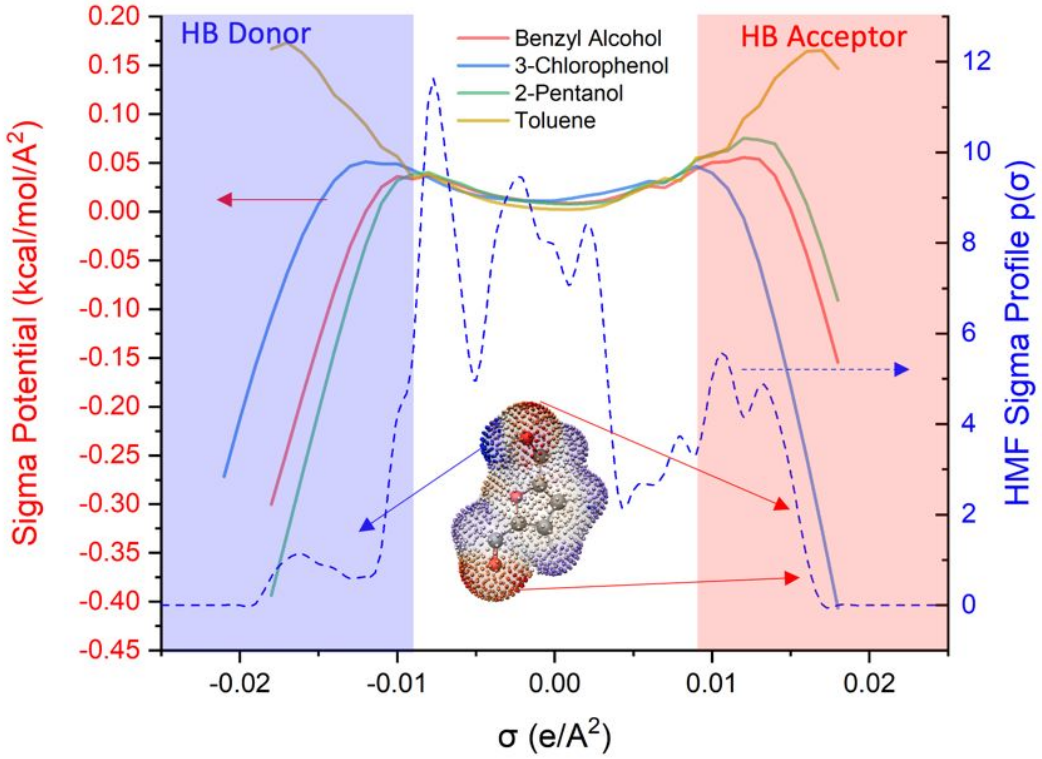

Figure 9. Sigma potential (solid lines) for solvent-rich phases of solvent-water systems at 298 K and pure HMF sigma profile (blue dash line). The abscissa illustrates the screening charge density of molecular surface segments. Note the highly positive ($\sigma > 0.00854$ e/Å^2) regime corresponds to the oxygen atoms acting as hydrogen bond acceptors.

Conclusions

We present a comprehensive solvent selection framework for aqueous-organic reactive extraction using the multiscale COSMO-RS model followed by an extensive experimental validation in select solvents of various homologous series. We apply the model to HMF produced in acid-catalyzed dehydration of fructose. Model predictions of partition coefficients and mutual solubilities of one solvent in the other are typically within a factor of 2 from experimental data, except for acids where deviations are larger possibly due to acid dissociation. Our data indicates the COSMO-RS model is semi-quantitatively predictive and excellent for screening purposes.

Model predictions across >2,500 water-solvents identify that many aromatic substituted amines and phenols possess high $P_{HMF} > 10$ (298 K) and improve partitioning by more than an order of magnitude compared to typical solvents used in prior work. The single-largest comprehensive experimental dataset presented (54 water-solvent pairs spanning molecules across different homologous series) establishes the highest reported experimental P_{HMF} at 298 K in 3-chlorophenol (57.1). We also evaluated P_{LA}, P_{FA}, and $P_{Fructose}$ for the other key products and the reactant. High separation selectivity $\alpha_{HMF/Fructose}$ is generally observed with a strong correlation between P_{HMF} and P_{LA} due to their chemical similarity. The partition coefficients of HMF and FA or fructose are though weakly correlated. Our data indicates that solvents that extract selectively HMF also extract LA.

Mutual solubility data reveals high-P_{HMF} organic solvents contain considerable water, whereas high fructose concentration leads to a modest P_{HMF} increase across typical solvents. In contrast, the solubility of organic solvents in water is typically low. CHEM21-based safety, health, and environment (SHE) scores for solvent toxicity for all non-reactive biphasic solvents underline that

best performing solvents may not meet SHE criteria. This data underscores the need to consider the effect of mutual solubility of solvents, their cost, and the SHE criteria in a combined, multi-objective optimization-based technoeconomic analysis.

Unlike biphasic separation at room temperature, reactive extraction happens at relatively high reaction temperatures, and solvent selection requires knowledge of temperature effects. We provide the first direct evaluation of P_{HMF} and separation factors between HMF, LA, and FA at reaction relevant temperatures through *in situ* sampling, preserving the phase composition at high temperatures after sampling. Our results show that increasing temperature leads to considerable reduction of P_{HMF} in high performing substituted phenols, moderate changes in typical solvents, along with a decrease in separation factors, and underscore the importance of reporting solute partition coefficients at relevant process temperatures, unlike the *status quo* in sugar dehydration literature. Finally, we augment the separation metric with solvent thermal stability and HMF compatibility data in a hierarchical manner to enable efficient solvent screening under reaction conditions. This methodological innovation rules out reactive amines, certain phenols, aldehydes, and organic acids as potential extractants despite giving favorable separations. We attribute the high P_{HMF} of best solvents in part to favorable hydrogen bond interactions with HMF, which can be investigated by molecular dynamics and/or middle to far IR studies in the future.

The findings in this work highlight the following hierarchical guidelines for solvent selection: (1) Screen solvents at room temperature based on separation performance to maximize product yields and minimize solvent volume. This criterion should, in general, improve economics but also energy consumption and environmental footprint. Screening is relatively easy to perform using the COSMO-RS platform. (2) Exploit temperature dependence of separation at relevant temperatures to further down-select solvents. (3) Determine solvent stability and compatibility with the reaction media, including products and catalysts at the reaction temperature. This task is currently performed experimentally on a smaller subset of solvents selected from the previous steps. (4) Evaluate high-performing solvents based on the SHE criteria using the CHEM21 recommendations. (5) Perform a comprehensive technoeconomic analysis on the entire process's cost, including that of the solvent, and the SHE criteria for the final selection of solvents. SHE criteria can be used as integer variables (acceptable vs. not acceptable solvent) or weighted into a multi-objective optimization. The current methodology and data can guide such future work.

Associated Content

Supporting Information

List of all solvents, Karl Fischer titration validation experiments for water-in-ketone standards, CHEM21-based solvent selection criteria for biphasic-capable non-reactive solvents, measured partition coefficients with and without fructose addition, mutual phase solubilities, time dependent P_{HMF} experiments with 2-chlorophenol at 298 K, *in situ* sampling setup at high temperature, comparison of mutual phase solubility and P_{HMF} between 298 K and 423 K, HPLC chromatographs for reactivity information between HMF and anilines, parity plots of predicted and experimentally measured P_{LA} and P_{FA} at 298 K and 423 K (including P_{HMF}), parity correlation between P_{HMF} and P_{LA} at 298 K and 423 K, effect of 20 wt% fructose in aqueous feed on P_{HMF} and water-in-organic solubility, variation of water-in-organic and organic-in-water solubilities with P_{LA}, P_{FA}, and $P_{Fructose}$, experimentally measured temperature dependence of P_{HMF}, P_{LA}, P_{FA}, and $P_{Fructose}$ between 298 K and 423 K, correlation between P_{HMF} and P_{LA}, P_{FA}, $P_{Fructose}$, respectively at 423 K, parity plots between full P_{HMF} predictions and P_{HMF} predictions discounting HB interactions at 298 and 423 K, together with P_{HMF} variation with and without HB temperature dependence at 423 K, and

an Excel document containing all COSMO-RS predictions are included in the Supporting Information.

Author Information

Corresponding Author
*vlachos@udel.edu

Author Contributions

Z.W. and S.B. contributed equally to the design and execution of the experiments, experimental data analysis, and computations. DGV provided the idea and oversaw the research. The manuscript was written by all authors. All authors approve the final version of the manuscript.

Conflicts of Interest

There are no conflicts to declare.

Acknowledgments

This work was supported in part by the RAPID manufacturing institute via the Department of Energy (DOE) Advanced Manufacturing Office (AMO), award number DE-EE0007888-7.6. RAPID projects at the University of Delaware are also made possible in part by funding provided by the State of Delaware. The Delaware Energy Institute gratefully acknowledges the support and partnership of the State of Delaware in furthering the essential scientific research being conducted through the RAPID projects.

References

1. K. Kohli, R. Prajapati and B. K. Sharma, *Energies*, 2019, **12**, 233.
2. J. J. Bozell and G. R. Petersen, *Green Chemistry*, 2010, **12**, 539-554.
3. S. Takkellapati, T. Li and M. A. Gonzalez, *Clean Technol Environ Policy*, 2018, **20**, 1615-1630.
4. M. Dusselier, M. Mascal and B. F. Sels, in *Selective Catalysis for Renewable Feedstocks and Chemicals*, ed. K. M. Nicholas, Springer International Publishing, **2014**, DOI: 10.1007/128_2014_544.
5. Y. Román-Leshkov and J. A. Dumesic, *Topics in Catalysis*, 2009, **52**, 297-303.
6. C. Sievers, I. Musin, T. Marzialetti, M. B. Valenzuela Olarte, P. K. Agrawal and C. W. Jones, *ChemSusChem*, 2009, **2**, 665-671.
7. T. Werpy and G. Petersen, *Top Value Added Chemicals from Biomass: Volume I -- Results of Screening for Potential Candidates from Sugars and Synthesis Gas*, Report DOE/GO-102004-1992, National Renewable Energy Lab., Golden, CO (US), **2004**.
8. A. A. Rosatella, S. P. Simeonov, R. F. M. Frade and C. A. M. Afonso, *Green Chemistry*, 2011, **13**, 754-793.
9. J. N. Chheda, Y. Román-Leshkov and J. A. Dumesic, *Green Chemistry*, 2007, **9**, 342-350.

10. Y. Román-Leshkov, J. N. Chheda and J. A. Dumesic, *Science*, 2006, **312**, 1933-1937.
11. B. F. M. Kuster, *Starch - Stärke*, 1990, **42**, 314-321.
12. D. Steinbach, A. Kruse, J. Sauer and P. Vetter, *Energies*, 2018, **11**, 15.
13. T. D. Swift, C. Bagia, V. Choudhary, G. Peklaris, V. Nikolakis and D. G. Vlachos, *ACS Catalysis*, 2014, **4**, 259-267.
14. T. G. Bonner, E. J. Bourne and M. Ruszkiewicz, *Journal of the Chemical Society*, 1960, DOI: 10.1039/jr9600000787, 787-791.
15. R. M. Musau and R. M. Munavu, *Biomass*, 1987, **13**, 67-74.
16. D. W. Brown, A. J. Floyd, R. G. Kinsman and Y. Roshanali, *J. Chem. Technol. Biotechnol.*, 1982, **32**, 920-924.
17. H. H. Szmant and D. D. Chundury, *J. Chem. Technol. Biotechnol.*, 1981, **31**, 135-145.
18. S. Hu, Z. Zhang, Y. Zhou, B. Han, H. Fan, W. Li, J. Song and Y. Xie, *Green Chemistry*, 2008, **10**, 1280-1283.
19. S. Hu, Z. Zhang, Y. Zhou, J. Song, H. Fan and B. Han, *Green Chemistry*, 2009, **11**, 873-877.
20. C. Moreau, A. Finiels and L. Vanoye, *Journal of Molecular Catalysis A: Chemical*, 2006, **253**, 165-169.
21. X. Qi, M. Watanabe, T. M. Aida and R. L. Smith Jr, *ChemSusChem*, 2009, **2**, 944-946.
22. F. Ilgen, D. Ott, D. Kralisch, C. Reil, A. Palmberger and B. König, *Green Chemistry*, 2009, **11**, 1948-1954.
23. L. C. Blumenthal, C. M. Jens, J. Ulbrich, F. Schwering, V. Langrehr, T. Turek, U. Kunz, K. Leonhard and R. Palkovits, *ACS Sustainable Chemistry & Engineering*, 2016, **4**, 228-235.
24. D. Mercadier, L. Rigal, A. Gaset and J. P. Gorrichon, *J. Chem. Technol. Biotechnol.*, 1981, **31**, 489-496.
25. J. Esteban, A. J. Vorholt and W. Leitner, *Green Chemistry*, 2020, **22**, 2097-2128.
26. B. Saha and M. M. Abu-Omar, *Green Chemistry*, 2014, **16**, 24-38.
27. L. Rigal and A. Gaset, *Biomass*, 1983, **3**, 151-163.
28. C. Fan, H. Guan, H. Zhang, J. Wang, S. Wang and X. Wang, *Biomass and Bioenergy*, 2011, **35**, 2659-2665.
29. C. García-Sancho, I. Fúnez-Núñez, R. Moreno-Tost, J. Santamaría-González, E. Pérez-Inestrosa, J. L. G. Fierro and P. Maireles-Torres, *Applied Catalysis B: Environmental*, 2017, **206**, 617-625.
30. B. Kuster and H. Steen, *Starch - Stärke*, 1977, **29**, 99-103.
31. S. Xu, X. Yan, Q. Bu and H. Xia, *RSC Advances*, 2016, **6**, 8048-8052.
32. L. Yang, X. Yan, S. Xu, H. Chen, H. Xia and S. Zuo, *RSC Advances*, 2015, **5**, 19900-19906.
33. E. Nikolla, Y. Román-Leshkov, M. Moliner and M. E. Davis, *ACS Catalysis*, 2011, **1**, 408-410.
34. L. Atanda, A. Silahua, S. Mukundan, A. Shrotri, G. Torres-Torres and J. Beltramini, *RSC Advances*, 2015, **5**, 80346-80352.
35. L. Atanda, M. Konarova, Q. Ma, S. Mukundan, A. Shrotri and J. Beltramini, *Catalysis Science & Technology*, 2016, **6**, 6257-6266.
36. A. Klamt, V. Jonas, T. Bürger and J. C. W. Lohrenz, *The Journal of Physical Chemistry A*, 1998, **102**, 5074-5085.
37. A. Klamt, *Journal*, **2005**.

38. J. Scheffczyk, L. Fleitmann, A. Schwarz, M. Lampe, A. Bardow and K. Leonhard, *Chemical Engineering Science*, 2017, **159**, 84-92.
39. C. C. Pye, T. Ziegler, E. van Lenthe and J. N. Louwen, *Canadian Journal of Chemistry*, 2009, **87**, 790-797.
40. AMS 2019.3 COSMO-RS, SCM, http://www.scm.com, (accessed 5/10/2020, 2020).
41. Y. Román-Leshkov, C. J. Barrett, Z. Y. Liu and J. A. Dumesic, *Nature*, 2007, **447**, 982-985.
42. Z. Yuan, Y. Zhang and C. Xu, *RSC Advances*, 2014, **4**, 31829-31835.
43. Y. J. Pagán-Torres, T. Wang, J. M. R. Gallo, B. H. Shanks and J. A. Dumesic, *ACS Catalysis*, 2012, **2**, 930-934.
44. E. I. Gürbüz, S. G. Wettstein and J. A. Dumesic, *ChemSusChem*, 2012, **5**, 383-387.
45. M. Kleinert and T. Barth, *Chemical Engineering & Technology*, 2008, **31**, 736-745.
46. The CHEM21 solvent selection guide interactive tool: solvent ranking, http://learning.chem21.eu/methods-of-facilitating-change/tools-and-guides/solvent-selection-guides/interactive-tool-chem21-guide/, (accessed November 4, 2020).
47. A. Klamt and F. Eckert, *Fluid Phase Equilibria*, 2000, **172**, 43-72.